High Resolution Solid State NMR in Liquid. IV. ^{1}H NMR Study of Terephthalic Acid Nano-Particles

Naoki Satoh,*,# Akira Naito,† and Keisaku Kimura†

Kao Institute for Fundamental Research, Kao Corporation,
2606 Akabane, Ichikai-machi, Haga-gun, Tochigi 321-34

†Faculty of Science, Himeji Institute of Technology, Kanaji, Kamigohri-cho, Akou-gun, Hyogo 678-15

(Received December 27, 1994)

High-resolution ^{1}H NMR spectra of terephthalic acid (TPA) ultrafine particles (UFP's) were obtained under the conditions of rapid Brownian motion of UFP's in liquid CCl_4 (UFP-NMR method). Six signals were resolved in the range of 6.85 to 7.65 ppm with respect to an tetramethylsilane. These were assigned to aromatic protons, even though only a single signal at 8.15 ppm was obtained from molecular dispersion of TPA in acetone. TPA-UFP dispersions were prepared by a vacuum evaporation technique combined with a cold matrix-isolation method. Particle sizes obtained were ca. 15 nm by a dynamic laser scattering method. The results from UFP-NMR method are discussed in conjunction with those from solid state ^{1}H NMR via a CRAMPS method and with a conventional liquid state NMR of TPA.

Solid-state NMR, especially with high-resolution techniques, is widely used to obtain detailed information on both structure and dynamics for a varieties of substances such as polymers, organic crystals, zeolites, and biological tissues. In recent years structural studies using solid state NMR techniques have been extensively reported in various fields of science, such as physics, chemistry, biology, and medicine.[1] It can be said, therefore, that solid state NMR has become an important technique as a powerful, but also a common tool for analytical technique. NMR spectral lines of solid-state samples are, in general, broad due to the presence of anisotropic interactions such as a magnetic dipole–dipole interaction, chemical shielding interaction, quadrupole interaction, etc. It is inevitable to reduce the broad line width in order to get useful NMR parameters such as chemical shifts of individual nuclei, multiplet of lines, and so forth.

In order to obtain one dimensional high-resolution NMR spectra, two different ideas of averaging technique have been developed, one is the averaging in the spin space and the other, that in the real space. In the former, multipulse averaging and high power heteronuclear decoupling are included. The latter can be further classified into two classes as for sample rotation techniques, artificial sample rotation around the fixed axis, and the random reorientation of samples. In the former category, magic angle sample spinning (MAS NMR) technique is applied to obtain high-resolution signals for dilute nuclei such as ^{13}C, ^{15}N, and ^{29}Si. Fast spinning MAS technique (with spinning speed in excess of 20 kHz) has been further developed to obtain high-resolution signals for abundant nuclei.[2] Recently it was reported that second order-broadening due to quadrupole interaction can be eliminated by means of double-rotating (DOR)[3] and dynamic angle spinning (DAS).[4] Not being sufficient as for abundant nuclei with large gyromagnetic ratio, spinning rate of sample rotation is limited by hardware so far. In order to obtain higher signal-resolution, MAS method is often combined with the multipulse sequences for abundant nuclei such as ^{19}F and ^{1}H.[5] However, satisfactory resolution has not yet been obtained even by the use of these techniques, especially for abundant nuclei such as protons. It is still quite difficult to achieve high-resolution NMR for protons in solids if a proton nucleus is surrounded by abundant proton nuclei having large magnetic dipoles. In such a case the decoupling technique which is effective for dilute spin systems can not be used, since both magnetic moments of the targeting proton and the surrounding protons are simultaneously excited by the decoupling irradiation. High-resolution solid-state ^{1}H NMR is, for this reason, one of the challenging goals for current NMR science. On the other side, random averaging technique for sample rotation has been scarcely developed.

Rapid and random motions of nuclei in a solid suppress these broadening effects,[6] which is well-known as motional narrowing. The present authors have reported that Brownian motion of nanometer-sized particles dispersed in a liquid phase provides well-resolved

#Present Address: Tokyo Research Laboratories, Kao Corporation, 1-3 Bunka 2-Chome, Sumida-Ku, Tokyo 131.

high-resolution NMR spectra for solid-state samples, which we have named "UFP (ultrafine particle)-NMR" in the first report of this series.[7] One of the advantages of the UFP-NMR method is that one can obtain information on solid surfaces without the need of high vacuum conditions as required in most other techniques. We demonstrated by ^{27}Al NMR that a signal from surfaces of AlF_3 clusters dispersed in methanol changed by addition of water.[8] Moreover, from changes in chemical shift of ^{27}Al, it was found that ionic character of Al–F bonding decreased from bulk to UFP's, being comparable with the results of X-ray photoelectron spectroscopy (XPS).[8] Another merit of UFP-NMR is that the motional narrowing can be expected to provide high-resolution spectra irrespective of their origin of the broadening. Very recently we have reported that UFP-NMR is applicable to high-resolution magnetic resonance of nuclei surrounded by homonuclear abundant spins in solids, namely, high-resolution solid-state ^{1}H NMR.[9] High resolution solid state ^{1}H NMR from UFP's of terephthalic acid (TPA) dispersed in carbon tetrachloride (CCl_4) were demonstrated in a previous report of this series.[9] TPA-UFP was chosen as a test material for UFP-^{1}H NMR because TPA is chemically stable against thermal treatments such as sublimation. Low solubility of TPA to conventional solvents is also important to stabilize a UFP state. In this report, we discuss changes in chemical shift of TPA UFP from those of both bulk and molecular state of TPA, and also discuss the width of NMR lines of TPA UFP taking the size of particles into consideration.

Although various preparation methods of both inorganic and metallic nanometer-sized particles have been established, few studies have been reported as for an effective technique to prepare organic ones. Hence, preparation of organic UFP's is itself a new challenge. We report precisely a novel method to prepare stable dispersions of organic UFP's with a diameter of ca. 10 nm. Well-resolved signals were obtained from aromatic protons of TPA when TPA-UFP's were dispersed in CCl_4. The results from UFP-NMR method are discussed in conjunction with those from solid state ^{1}H NMR via the CRAMPS method and with a conventional liquid state NMR.

Experimental

Preparation of Organic UFP's. Guaranteed grade of TPA was purchased from Tokyo Kasei Ltd. and was purified twice by sublimation in vacuum conditions being held at 270 °C. Dispersing liquid CCl_4 (Spectro-grade) was purchased from Wako Chemicals Co., Ltd. and was purified by 4A molecular sieves and by active carbon powder.

Preparation of a stable TPA UFP dispersion is based on an island formation of deposit on a cold matrix by the vacuum evaporation method. Several solvents such as dichloromethane, benzene, carbon tetrachloride, methanol, acetone, etc. were tested whether they were appropriate for dispersing medium. However, none of them was able to disperse TPA UFP's at all by a single component, or TPA was too soluble in some solvents to stabilize UFP's. Although surface active agents are effective to stabilize nanometer-sized particles in a liquid,[10] surfactants conventionally used are not suitable in this case to disperse UFP's because of the following reasons. Surfactant molecules have generally a large molecular weight and a molecular length. Adsorption of surfactant molecules leads to growth in size of UFP's, which is disadvantageous for motional narrowing by means of Brownian motion of UFP's. Moreover, proton signals of surfactants may disturb signals from UFP's. Deuterated acetone (acetone-d_6) or deuterated methanol (methanol-d_4) was thus chosen as a dispersing reagent because of both their small molecular sizes and their large solubilities against TPA, suggesting their high affinities to TPA. CCl_4 was the best as a dispersing medium with these dispersing agents, because solubilities of TPA to CCl_4, CCl_4/acetone-d_6 mixture and CCl_4/methanol-d_4 mixture are low enough to stabilize UFP-state and to suppress molecular signals of TPA. The schematic diagram of preparation chamber is illustrated in Fig. 1(a). Purified bulk TPA was settled in an aluminum coated heater. The glass chamber was once evacuated to less than 1.0×10^{-6} Torr (1 Torr=133.322 P_a) by a molecular turbo pump. The wall of the chamber was then cooled by liquid nitrogen in order to deposit a cold matrix of CCl_4. Evaporation of CCl_4 was continued for 90 s, which was followed by sublimation of TPA on the CCl_4 cold matrix. The amount of TPA deposited was controlled to ca. 4.0 nm with a quartz film thickness monitor, Sloan 200. Island like deposition of TPA was confirmed through TEM observations. After the sublimation of TPA, acetone-d_6 or methanol-d_4 was deposited on TPA particles for less than one second. These three deposition steps of CCl_4, TPA and dispersing reagent were repeated nine times in this order. The situation of stacking layers is schematically illustrated in Fig. 1(b). Liquid CCl_4 was then added on the cold matrix to adjust the concentration of acetone-d_6 or methanol-d_4 to be 1 vol% of total volume of the dispersion. Finally, the matrix was melted under the irradiation of ultrasonic wave (Fig. 1(c)). Although the dispersion was transparent, Tyndal scattering light was clearly observed by irradiation of a He–Ne laser. Dynamic laser scattering (DLS) measurements were carried out with an Ohtsuka ELS-800 for obtaining size distributions of UFP.

^{1}H NMR Measurements. ^{1}H NMR measurements on dispersion and liquid samples were carried out at the Institute for Molecular Science in Okazaki on a FT NMR spectrometer, JEOL GX400 using a probe for irradiation frequency of 399.8 MHz. Colloidal and liquid samples were sealed into a conventional 5-mm sample tube with 17 Hz sample spinning rate. Longitudinal relaxation time T_1 was measured by an inversion recovery method with a $180^\circ-\tau-90^\circ$ pulse sequence and transverse relaxation time T_2 by an CPMG (Carr–Purcell–Meiboom–Gill) method. In order to detect a signal from protons of carboxyl groups, UFP NMR measurements were also carried out at low temperature using cold nitrogen gas. 50 wt% mixture of $CDCl_3$ and CCl_4 was used for the low temperature measurements in order to avoid freezing.

The solid state ^{1}H NMR combining magic angle spinning with multiple-pulse sequence, CRAMPS (Combined Rotation and Multiple-Pulse Spectroscopy) method was carried

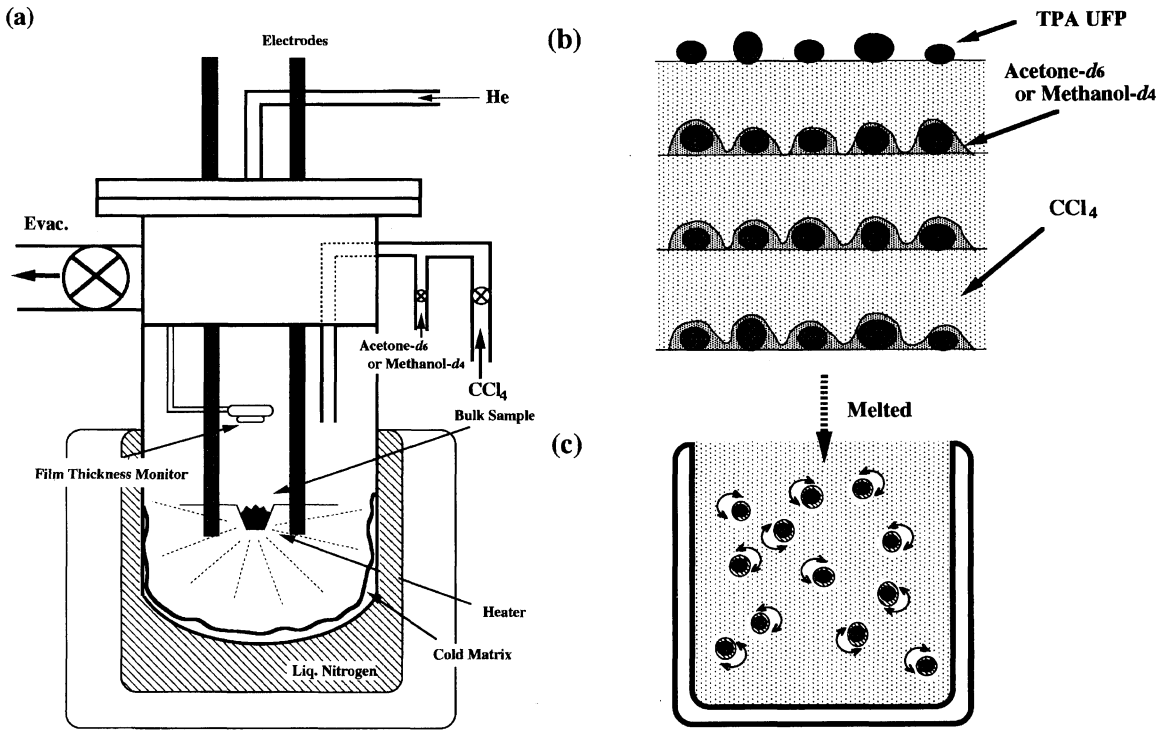

Fig. 1. The apparatus for the preparation of TPA UFP dispersion (a), an illustration of the UFP's in the cold matrix of CCl_4 (b), and the UFP's undergoing Brownian motion in liquid CCl_4 (c).

out at Faculty of Science, Himeji Institute of Technology. The CRAMPS NMR spectra were recorded on a CMX-400 type FT NMR spectrometer (Chemagnetics Ltd.) with a CRAMPS probe with BR-24 pulse-sequence.

Tetramethylsilane (TMS) was used as an external chemical shift reference standard for ^{1}H UFP NMR and methyl protons of L-alanine for CRAMPS method at 1.3 ppm lower field from TMS.[11]

Results and Discussion

NMR Signals from Ultrafine Particles of TPA. Figure 2(a) shows a number distribution of TPA UFP/Acetone-d_6/CCl_4, and Fig. 2(b) TPA UFP/Methanol-d_4/CCl_4 obtained by DLS measurements. Small particles with a diameter of ca. 15 nm were obtained in both systems. However, the Tyndal scattering was lost and no signal was obtained by DLS measurements when the evaporation of TPA was continued up to 230 nm in the preparation process. This fact suggests that there is a critical thickness such as percolation limit for obtaining UFP's above which island-like deposits grow into films. Tyndal scattering was also lost when dispersing agent was not used.

Figure 3 shows ^{1}H NMR spectra from aromatic protons of TPA in various states after 500 accumulation times. The colloidal dispersion of TPA UFP/acetone-d_6/CCl_4 provides six peaks, which are located at 6.85, 6.95, 7.08, 7.25, 7.50, and 7.65 ppm as seen in Fig. 3(a). The full widths at half maximum (FWHM) of six peaks were of the order of 0.1 ppm, i.e., 40 Hz. Similar six signals with an additional peak positioned at 8.15 ppm were appeared in the case of TPA UFP/methanol-d_4/CCl_4 system (Fig. 3(b)). The original signal from aromatic proton of TPA dissolved in acetone-d_6 is referenced in Fig. 3(e). Comparing Fig. 3(b) with (e), the signal at 8.15 ppm corresponds to that from molecularly dispersed TPA. Because of higher solubility of TPA to methanol than to acetone, small amount of TPA is supposed to dissolve into liquid phase in the TPA UFP/methanol/CCl_4 system. In all above spectra carboxyl protons were not observed.

The signals observed in the TPA UFP/dispersing reagent/CCl_4 systems (Figs. 3(a) and 3(b)) were significantly diminished or completely lost both when the dispersing reagents were not used on the preparation process and when TPA was deposited to more than 200 nm thickness. Figure 3(c) and (d) show ^{1}H NMR spectra from a TPA UFP (4 nm)/CCl_4 system and a TPA film (230 nm)/acetone-d_6/CCl_4 system, respectively. The signals observed in the UFP dispersions were dramatically weakened in both spectra being consistent with the results from DLS measurements. Furthermore, no signal was observed from TPA saturated acetone-d_6 diluted with 100 times or even with 2.5 times volumes of CCl_4. These results strongly suggest that the six signals observed in Fig. 3(a) and (b) originated from the dispersed TPA UFP's in CCl_4.

In order to confirm that the signals were certainly from TPA UFP's, the following approaches were employed. Firstly, the solvent of TPA UFP/acetone-d_6/CCl_4 was evaporated to obtain UFP powders of TPA, which were then dissolved again into acetone-d_6.

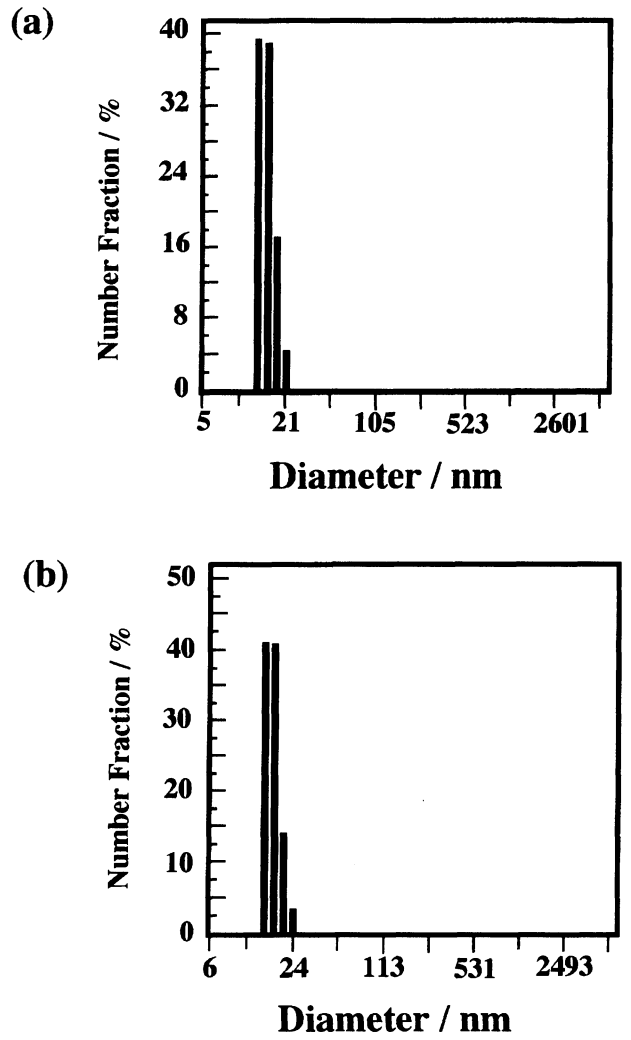

Fig. 2. The particle size distributions obtained by DLS measurement. (a) TPA UFP/acetone-d_6/CCl_4 and (b) TPA UFP/methanol-d_4/CCl_4.

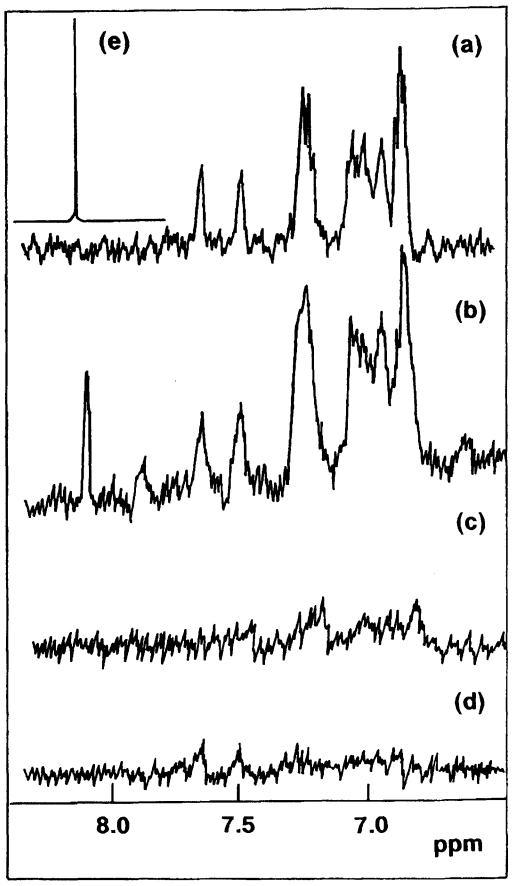

Fig. 3. ^{1}H NMR spectra of aromatic protons of TPA by a conventional NMR spectrometer. (a) TPA UFP (4.0 nm)/acetone-d_6/CCl_4, (b) TPA UFP (4.0 nm)/methanol-d_4/CCl_4, (c) TPA UFP (4.0 nm)/CCl_4, (d) TPA UFP (230.0 nm)/acetone-d_6/CCl_4 and (e) molecularly dispersed TPA in acetone-d_6.

During this process, UFP's are believed to completely dissolve into solvent or disperse into finer assemblies than UFP's, namely, cluster states. Figure 4(a) shows ^{1}H NMR of the resultant solutions. The six signals decreased in their intensities, sharpened in resolution and enhanced in signal to noise ratio, and a new peak indicating molecularly dissolved TPA alternatively developed at 8.15 ppm. It should be noted that the six signals did not distinguish completely even in pure acetone-d_6. Correspondingly, light scattering was still observed after this process. These facts suggest that TPA UFP's once prepared by the present method were quite stable against drying and redissolving processes and that their sizes became smaller than before. Therefore, we tried an additional sublimation of TPA UFP. The sample, TPA UFP/acetone-d_6/CCl_4 dispersion was once evacuated to remove solvents being followed by sublimation at 290 °C, and then the powder obtained was dissolved again in acetone-d_6. Whole processes were carried out in the same NMR sample tube to avoid any unexpected contamination. Figure 4(b) shows the spectrum of this resublimated sample. There is only a signal at 8.15 ppm from molecularly dissolved TPA. The strong peak at 5.6 ppm is due to an impurity in acetone-d_6. Coincidentally, the strong light scattering upon irradiation of a He–Ne laser was lost in the resublimated sample. These observations strongly support that the six peaks found in Fig. 3(a) and (b) are due to TPA UFP's. It is recognized that these six signals show additional fine structures which are particularly clear in Fig. 4(a). These fine structures may be caused by spin–spin couplings between protons. These fine structures (separation around 5—10 Hz) can never be seen in CRAMPS ^{1}H NMR because of the limited resolution.

Figure 5 shows the solid state ^{1}H NMR spectra of bulk TPA via CRAMPS method. The broad peak observed was centered at 7.3 ppm, which is 0.85 ppm (0.34 kHz) higher field than that of molecularly dispersed TPA and ranged over the same region with that of dispersed UFP. Therefore, it can be said that the dispersed UFP shows a character of bulk solid with ul-

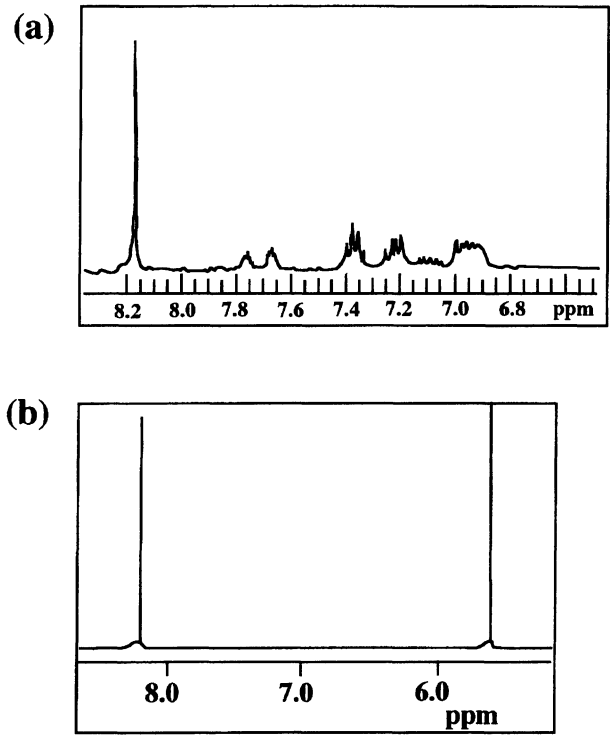

Fig. 4. ^{1}H NMR spectra of TPA in acetone-d_6. (a) After drying of TPA UFP/acetone-d_6/CCl_4 and (b) after resublimation of TPA UFP/acetone-d_6/CCl_4.

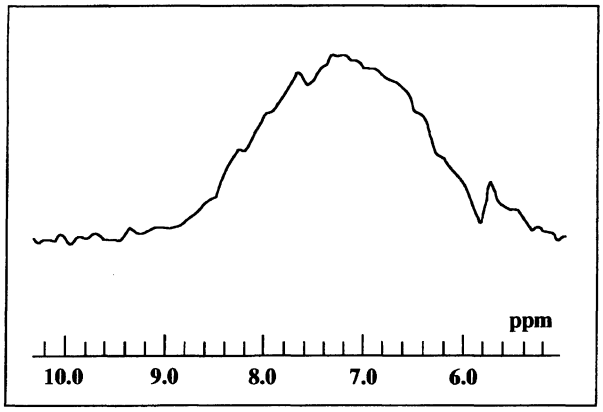

Fig. 5. Solid state ^{1}H NMR spectra of bulk TPA via CRAMPS method. Data was accumulated 118 times.

trahigh spectral resolution rather than a free molecule in a solution. However, the width (FWHM) of the CRAMPS peak reached 1.95 ppm, i.e., 0.78 kHz and the fine structures were hardly observed. In CRAMPS experiment, the line width for the compounds containing phenyl groups is usually larger than those without such groups because of large anisotropy in bulk magnetic susceptibility. The reported line width is usually around 800 Hz.[12]

Chemical shifts of aromatic protons varied from 8.15 to 6.85 ppm according to the state of TPA, i.e., molecular dispersion, UFP, and solid state. In molecularly dispersed state all of the four aromatic protons are equivalent providing single NMR peak, 8.15 ppm because of high-speed rotation of the carboxyl groups or high-speed exchange of the carboxyl protons between two carboxyl oxygens forming hydrogen bonding. In the solid state carboxyl groups of TPA are reported to be in a trans conformation according to crystallographic data.[13] Two types of aromatic protons of TPA are not already equivalent with each other in this state. Furthermore, two types of crystal forms, both of which are based on triclinic crystal, are reported.[13] Four signals, at most, can emerge as a result of this polymorphs of crystal structure of TPA and nonequivalence of aromatic protons in each unit cell. However, the other two signals are not explained at this stage. This deviation could be based on characteristics of small particles, such as large fraction of surface molecules and/or the third polymorphic form realized only in small particle.

Chemical shifts of aromatic ring protons in solid states are often reported in the higher field (shielded) region than those in solution state (molecular dispersion).[12] This may be due to the restriction of the carboxyl group rotation and the resultant decreasing in the deshielding effect. In Fig. 6, we show the development of the chemical shifts as a function of particle size, i.e. (a) bulk, (b) UFP, (c) cluster, and (d) molecule. From this figure, it is shown that the bulk peaks converge into the molecular peak via. UFP and cluster states; i.e. intermediate cases, b) and c) were observed between the two extremes, bulk and molecules, and furthermore, the

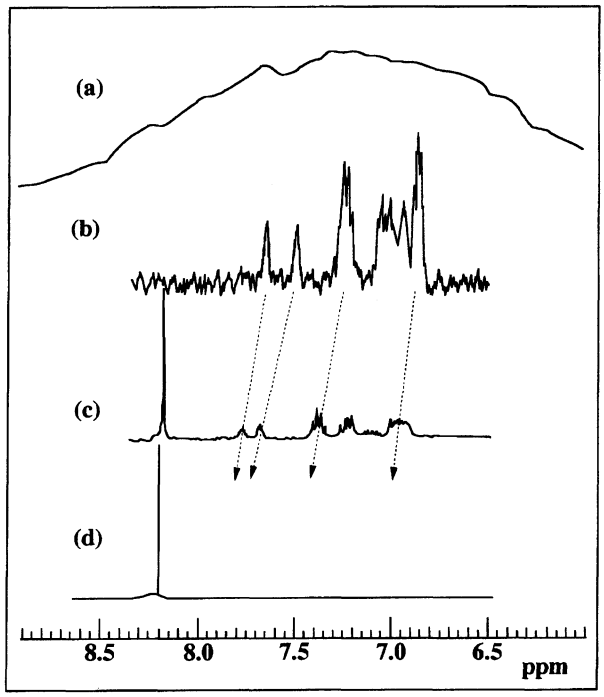

Fig. 6. Spectral change with decrease in size of TPA. (a) bulk, (b) UFP, (c) cluster (with molecule), and (e) molecule. Arrows in the figure denote changes in chemical shifts.

peaks from the UFP's (b) shifted to lower field in spectrum (c) (cluster with molecule), the degree of shifts depending on each peak. This fact suggests that the peaks are sensitive to a fraction of surfaces, namely, the larger the fraction of surfaces is, the lower field the chemical shift moves toward. In molecular state, where all atoms are exposed to surface, the chemical shift is located at the lowest field, 8.15 ppm.

Relaxation Time and Particle-Size. Because homonuclear dipole–dipole interaction is the main relaxation mechanism in the TPA UFP dispersions, particle sizes can be estimated by the measurement of relaxation times, T_1 and T_2, from respective signals. The ratio T_2/T_1 of the nucleus undergoing dipole–dipole relaxation is simply described as

$$\frac{T_2}{T_1} = 2\frac{1/(1+\omega^2\tau^2)+4/(1+4\omega^2\tau^2)}{3+5/(1+\omega^2\tau^2)+2/(1+4\omega^2\tau^2)}, \quad (1)$$

where, ω and τ are a Larmor frequency and a correlation time of molecular motion, respectively. Following Debye's theory of dielectric dispersion,[14] the rotational correlation time for a spherical particle undergoing Brownian motion can be expressed as[14,15]

$$\tau = \frac{4\pi\eta a^3}{3kT}, \quad (2)$$

where a is the radius of a particle, and other symbols have their usual meanings. The ratio of T_2/T_1 can be expressed only as a function of the particle size using relevant values for ω, η, and T which are decided as experimental conditions. Figure 7 shows the calculated ratio of relaxation time T_2/T_1 as a function of particle size. It is shown that extreme narrowing condition is realized below ca. 1.0 nm. Observed relaxation times of aromatic protons from TPA UFP/acetone-d_6/CCl_4 system are summarized in Table 1. The observed T_2/T_1 ratio ranged between 0.4 and 0.89. Particle size corresponding to the peaks were estimated through Fig. 7 and described in Table 1. Estimated diameters ranged between ca. 1 and 1.5 nm, which were one order smaller than that obtained by DLS measurements. One explanation for this discrepancy may be difference in observing size-region of UFP's between by NMR and by DLS. By means of NMR, the smaller the particles are, the more easily they are detected, which is just opposite to the case of DLS. The other explanation is more rapid reorientation of TPA UFP's than expected because of lubricant effect of the surface active molecules surrounding UFP's the viscosity of which is three times smaller

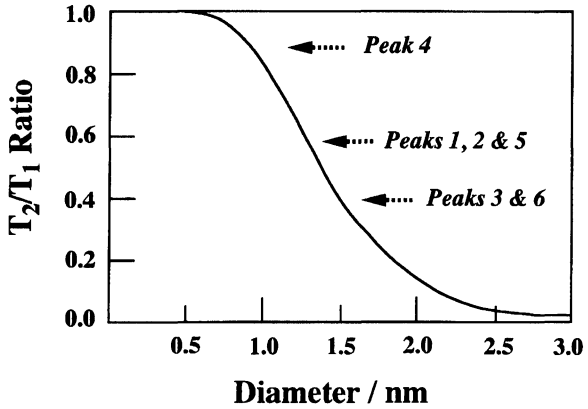

Fig. 7. Calculated curve of T_2/T_1 ratio of ^{1}H NMR as a function of diameter of a particle taking only dipole–dipole relaxation of protons into consideration with relevant values for ω, η, and T which was decided as experimental conditions. Peak numbers from 1 to 6 denote NMR signals located at 6.85, 6.95, 7.08, 7.25, 7.50, and 7.65 ppm, respectively.

than that of CCl_4. Israellachvili et al. found through their study of molecular tribology using surface force apparatus (SFA) that a trace amount of water or methanol in hydrophobic solvent dramatically reduces frictional force between mica surface and the solvent confined in a molecularly narrow space.[16] This decrease in frictional force between surface of TPA UFP and CCl_4 will cause effectively smaller viscosity in Eq. 2, and will be an origin of misleading particle size.

Temperature Dependence of NMR Signals from TPA. In order to detect NMR signals from carboxyl groups, samples were cooled down during NMR measurements. Figure 8(a) shows NMR signals from TPA UFP's dispersed in acetone-d_6(1)/$CDCl_3$ (49.5)/CCl_4 (49.5) observed at low temperature. At higher temperature than −20 °C, signals are hardly found around −13 ppm, where signals from carboxyl protons are expected. At −20 °C, however, a very weak signal was observed at 13.15 ppm. The signal became stronger and shifted to lower fields with decreasing temperature. At −50 °C, the signal was centered at 13.71 ppm, and at −78 °C, at 14.03 ppm (Fig. 8(a)). In Fig. 8(b), NMR spectra of molecularly dispersed TPA in cold acetone-d_6 are compared. Although similar changes were observed for both intensity and chemical shift, the peak was broader, located at higher field and observed at lower temperature, i.e., <-50 °C in

Table 1. NMR Parameters of TPA UFP's

Peak No.	1	2	3	4	5	6
Chemical Shift/ppm	7.65	7.50	7.25	7.08	6.95	6.80
T_1/ms	1587	1443	2164	1298	2453	2164
T_2/ms	866	866	866	1154	1443	866
T_2/T_1	0.546	0.600	0.400	0.899	0.588	0.400
Diameter D/nm	1.3	1.3	1.5	0.9	1.3	1.5

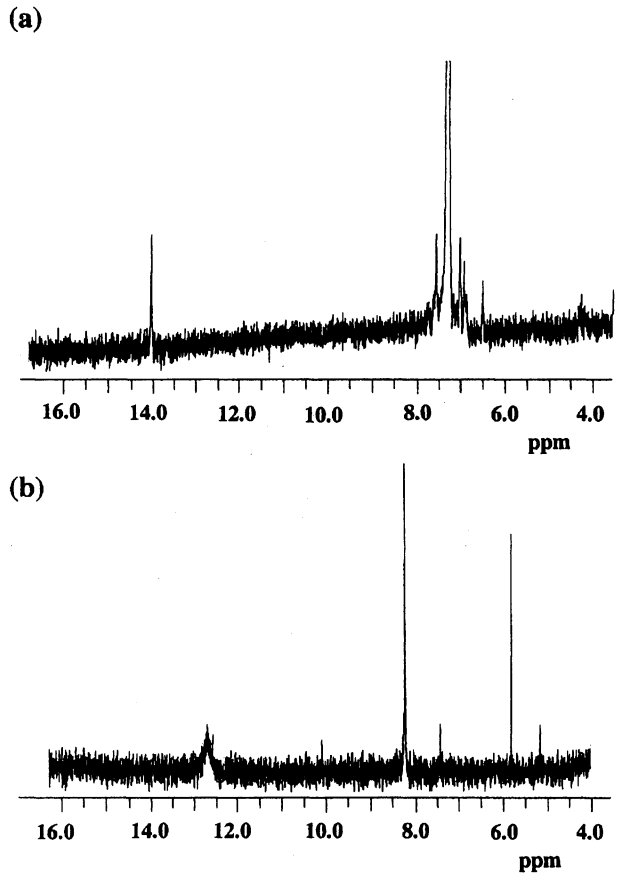

Fig. 8. (a) ^{1}H NMR spectrum of TPA UFP (4.0 nm)/Acetone-d_6/$CDCl_3$/CCl_4 observed at −78 °C. A strong signal from impurity of $CDCl_3$ overlaps upon the region from aromatic protons of UFP's. (b) ^{1}H NMR spectrum from molecularly dispersed TPA in acetone-d_6 observed at −75 °C. A strong signal at 8.2 ppm is from aromatic protons of TPA.

the case of molecularly dispersed TPA. Although this phenomena observed at lower temperature is not understood well at present, it may be interpreted in terms of the stability of hydrogen bond. Hydrogen bond in a solid is stabilized giving a low field shift in the NMR signal: The chemical shift of carboxyl proton increases with decrease in temperature. On the other hand, the chemical shift tendency in a molecularly dispersed TPA is not straightforward. In this case, we have to take account of the effect of temperature on both hydrogen bond and solvation. The chemical shift tendency on temperature of both UFP and molecularly dispersed TPA may be interpreted in terms of stabilization of the hydrogen bond. We leave it for future research.

We thank Professor H. Saito for permission of the measurement of CRAMPS NMR.

References

1) C. A. Fyfe, "Solid State NMR for Chemists," CFC Press, Canada (1983).
2) R. A. Wind, S. F. Dec, H. Lock, and G. E. Maciel, *J. Magn. Reson.*, **79**, 136 (1988).
3) Y. Wu, B. Q. Sun, A. Pines, A. Samoson, and E. Lippmaa, *J. Magn. Reson.*, **89**, 297 (1990).
4) K. T. Mueller, B. Q. Sun, G. C. Chingas, J. W. Zwanziger, T. Terao, and A. Pines, *J. Magn. Reson.*, **86**, 470 (1990).
5) M. Mehring, "Principles of High Resolution NMR in Solids," 2nd ed, Springer, Berlin (1983).
6) J. P. Jesinowski, *J. Am. Chem. Soc.*, **103**, 6266 (1981).
7) K. Kimura and N. Satoh, *Chem. Lett.*, **1989**, 271.
8) N. Satoh and K. Kimura, *J. Am. Chem. Soc.*, **112**, 4688 (1990).
9) N. Satoh and K. Kimura, *Chem. Lett.*, **1994**, 2155. The first report of the ^{1}H UFP NMR method was presented at the International Congress of Pacific Basin Societies (1989): Abstr., *Phys. Chem.*, **9**, 306 (1989).
10) N. Satoh and K. Kimura, *Bull. Chem. Soc. Jpn.*, **62**, 1758 (1989).
11) G. Scheler, U. Haubenreisser, and H. Rosenberger, *J. Magn. Reson.*, **44**, 134 (1981).
12) C. E. Bronnimann, B. L. Hawkins, M. Zhang, and G. E. Maciel, *Anal. Chem.*, **60**, 1743 (1988).
13) M. Bailey and J. C. Brown, *Acta Crystallogr.*, **22**, 387 (1967).
14) A. Abragam, "The Principles of Nuclear Magnetism," Oxford University Press, London and New York (1961), Chap. XIII.
15) P. Debye, "Polar Molecules," Dover, New York (1929), Chap. 5.
16) M. L. Gee, P. M. McGuiggan, J. N. Israelachvili, and A. M. Homola, *J. Chem. Phys.*, **93**, 1895 (1990).